



# Response of global evaporation to major climate modes in historical and future CMIP5 simulations

Thanh Le<sup>1,2</sup>, Deg-Hyo Bae<sup>1,2</sup>

<sup>1</sup>Department of Civil & Environmental Engineering, Sejong University, Seoul, South Korea

5 <sup>2</sup>Center for Climate Change Adaptation for Water Resources, Sejong University, Seoul, South Korea

*Correspondence to:* Deg-Hyo Bae (dhbae@sejong.ac.kr)

**Abstract.** Climate extremes, such as floods and droughts might have severe economic and societal impacts. Given the high costs associated with these events, developing early warning systems are of high priority. Evaporation, which is driven by around 50% of solar energy absorbed at surface of the Earth, is an important indicator of global water budget, monsoon precipitation, drought monitoring and hydrological cycle. Here we investigate the response of global evaporation to main modes of interannual climate variability, including the Indian Ocean Dipole (IOD), the North Atlantic Oscillation (NAO) and the El Niño-Southern Oscillation (ENSO). These climate modes may have influence on temperature, precipitation, soil moisture, wind speed, and are likely to have impacts on global evaporation. We utilized data of historical simulations and RCP8.5 future simulations derived from Coupled Model Intercomparison Project Phase 5 (CMIP5). Our results indicate that ENSO is an important driver of evaporation for many regions, especially the tropical Pacific. The significant IOD influence on evaporation is limited in western tropical Indian Ocean while NAO is more likely to have impacts on evaporation of the North Atlantic European areas. Land evaporation is found to be less sensitive to considered climate modes compared to oceanic evaporation. The spatial influence of major climate modes on global evaporation is slightly more significant for NAO and the IOD while slightly less significant for ENSO in the 1906–2000 period compared to the 2006–2100 period. This study allows us to obtain insight about the predictability of evaporation, and hence, may improve the early warning systems of climate extremes and water resources management.

**Keywords:** ENSO; IOD; NAO; Evaporation; CMIP5; Water resources management;

## 1 Introduction

The North Atlantic Oscillation (NAO; e.g., Hurrell et al., 2003), the Indian Ocean Dipole (IOD; Saji et al., 1999; Webster et al., 1999), and the El Niño-Southern Oscillation (ENSO; e.g., Bjerknes, 1969; Neelin et al., 1998) are major modes of global climate variability. These climate modes may have influence on surface temperature (e.g., Arora et al., 2016; Leung & Zhou, 2016; Sun et al., 2016; Thirumalai et al., 2017; Wang et al., 2017), precipitation (Dai and Wigley, 2000), soil moisture (Nicolai-Shaw et al., 2016), humidity (Hegerl et al., 2015) and wind speed (Hurrell et al., 2003; Yeh et al., 2018), and are likely to have impacts on global evaporation and transpiration (hereafter simply referred as ‘evaporation’). Evaporation,



30 which is driven by around 50% of solar energy absorbed at surface of the Earth (Cavusoglu et al., 2017; Jung et al., 2010), is  
an important indicator of global water budget, monsoon precipitation, drought monitoring and hydrological cycle (Friedrich  
et al., 2018; Kitoh, 2016; Lee et al., 2019; Van Osnabrugge et al., 2019; Son and Bae, 2015). Additionally, changes in global  
evaporation are expected to feedback on global and regional climate. For example, land evaporation is shown to have  
influences on carbon cycles (Cheng et al., 2017), cloud cover (Teuling et al., 2017) and air temperature (Miralles et al.,  
35 2012).

While previous studies emphasize the importance of ENSO on global evaporation (e.g., Miralles et al., 2013), the roles of the  
IOD and NAO remain elusive. In addition, the future influence of these climate modes on global evaporation under warming  
environment remain unclear. Climate change and rising temperature might increase surface evaporation (Miralles et al.,  
2013), and thus, might reduce global water availability and cause change in hydrological cycle (e.g., Naumann et al., 2018).  
40 Moreover, previous works mainly address the connection between individual climate mode and evaporation, however, the  
role of other climate modes might not be included in the analyses. As long term and reliable evaporation data is lacking (e.g.,  
Hegerl et al., 2015; Miralles et al., 2016), climate model simulations provide additional opportunity to examine the impacts  
of main climate modes on global evaporation. Besides, evaluating the models' consistency in reproducing the impacts of  
internal climate variability on evaporation is important for understanding the difference between models.

45 Here we investigate the causal impacts of major climate modes (i.e. ENSO, IOD and NAO) on global terrestrial and oceanic  
evaporation in CMIP5 model simulations for the 1906-2000 and the 2006-2100 periods. For this investigation, we use  
multivariate predictive models and tests of Granger causality which consider the simultaneous impact of climate modes on  
global evaporation (see Methods section 2.2).

## 2 Data and Methods

### 50 2.1 Data

The data used in the present study was obtained from Coupled Model Intercomparison Project Phase 5 (CMIP5). We employ  
data of historical simulations (experiment name 'historical' in CMIP5) and future simulations with high-emissions climate  
change scenario (experiment name Representative Concentration Pathway [RCP] 8.5 scenario, 'rcp85') (Taylor et al., 2012).  
The starting year of historical simulations is roughly 1850 and the ending year is roughly 2005 while the starting year of  
55 future simulations is roughly 2006 and the ending year is roughly 2100. In our analyses, we only use the data for the 1906-  
2000 historical period as a reference for the future period 2006-2100. Using other data period with similar length (i.e., 95  
years) does not alter the results and conclusions. We use different data variables, including monthly sea level pressure (i.e.,  
'psl' in CMIP5 datasets), sea surface temperature (i.e., 'ts'), and evaporation (i.e., 'evspsbl'). For each model, we only utilize  
one simulation (i.e., 'r1i1p1'). The models employed in this study are listed in Table S1 (Supplement). Terrestrial  
60 evaporation is the flux of water at surface into the atmosphere due to transformation of both solid and liquid phases to vapor



(from vegetation and underlying surface). Most of climate models do not provide separately the data of evaporation from canopy (i.e. transpiration) and water evaporation from soil (i.e. evaporation).

There might exist model biases in simulating ENSO (e.g. Taschetto et al., 2014), the IOD (Chu et al., 2014; Weller and Cai, 2013), NAO (Gong et al., 2017; Lee et al., 2018) and there is uncertainty in capability of land surface models in modeling  
65 evaporation (Mueller & Seneviratne, 2014; Wang & Dickinson, 2012). However, CMIP5 data is useful and provides additional understanding about the connections between major climate modes and global evaporation.

## 2.2 Methods

The NAO index (Hurrell et al., 2003) is computed as the first empirical orthogonal function (EOF) of boreal winter (DJF) sea level pressure (SLP) anomalies in the North Atlantic area (90°W-40°E, 20°-70°N). We compute the dipole mode index  
70 (DMI) (Saji et al., 1999) as the discrepancy of SST anomalies between the western tropical Indian Ocean (50°E-70°E; 10°N-10°S) and the south-eastern tropical Indian Ocean (90°E-110°E; 0°N-10°S) in the boreal fall (SON). We define the ENSO index as the average sea surface temperature (SST) anomalies in the Niño 3.4 region (120°W-170°W; 5°N-5°S) during boreal winter. We include ENSO, IOD and NAO in our analyses as these indices are three major climate modes of tropical Pacific, tropical Indian and North Atlantic Oceans.

75 We evaluate the causal effects of a climate mode (i.e., NAO or DMI or ENSO) on evaporation by using the following predictive model (e.g., Mosedale et al., 2006):

$$X_t = \sum_{i=1}^p \alpha_i X_{t-i} + \sum_{i=1}^p \beta_i Y_{t-i} + \sum_{j=1}^m \sum_{i=1}^p \delta_{j,i} Z_{j,t-i} + \varepsilon_t \quad (1)$$

where  $X_t$  is the annual (or seasonal) evaporation for year  $t$ ,  $Y_t$  is the selected index (i.e., ENSO or NAO or DMI) for evaluating the causal effects on evaporation for year  $t$ ,  $Z_{j,t}$  is the confounding variable  $j$  for year  $t$ ,  $p \geq 1$  is the order of the  
80 causal model, and  $m$  is total number of confounding variables. The optimal orders are normally less than 8 in our analysis, suggesting that the impact of major climate modes on evaporation is evaluated at inter-annual time scales. Confounding variables (e.g., if NAO is the selected index of possible causal influence on evaporation, the confounding variables are DMI and ENSO) may have impacts on the links between selected index and global evaporation. There are two form of confounding variables in our analysis, hence,  $m$  is equal to 2 in equation (1). The regression coefficients  $\alpha_i$ ,  $\beta_i$  and  $\delta_{j,i}$  and the  
85 noise residuals  $\varepsilon_t$  are computed by using multiple linear regression analysis and least squares method. All climate indices and evaporation data are normalized and detrended.

We apply test of Granger causality for the predictive model described in equation (1). Specifically, in order to assess the causal influence from  $Y$  to  $X$ , we compute the probability of the null hypothesis for an absence of Granger causality from  $Y$  to  $X$ . Additional information on the test of Granger causality are explained in earlier works (e.g., Le, 2015; Le et al., 2016).

90 The techniques employed in the present study provide robust assessment about the causal influence of considered climate



mode on global evaporation. In addition, these approaches account for the concurrent influence of confounding variables and hence, provide more realistic evidence of the response of global evaporation to major climate modes.

### 3 Results and discussions

#### ENSO influence on evaporation

95 The probability maps of no Granger causality between ENSO and global evaporation for the periods 1906–2000 and 2006–  
2100 are shown in Figure 1. In both periods, ENSO is more likely to have influence on evaporation of different regions  
(highlighted in blue shades) in both hemispheres, including middle Asia (regions closed to Caspian Sea, details are shown in  
Figure S1a in the Supplement), Indian Oceans, Indochina Peninsula, Australia (Figure S1b), tropical Pacific and northeastern  
South America (i.e. Amazonia, Figure S1c) and the Pacific coast of America (Figure S1d). There is high agreement between  
100 models (indicated by stippling in Figure 1) in simulating ENSO–evaporation connection of these regions. Specifically, high  
agreement of climate models in teleconnection between ENSO and tropical oceans evaporation implies that models can  
simulate the impacts of ENSO on evaporation. ENSO might indirectly influence global evaporation by modulating regional  
climate factors associated with evaporation processes. For example, ENSO significantly influence near surface wind, which  
is the main contributor of change in evaporation (Xing et al., 2016). The ENSO impacts on large part of tropical Pacific  
105 Ocean are robust at 5% and 10% significance levels (here we reject the null hypothesis of the absence of Granger causal  
effects between ENSO and evaporation at 5% and 10% significance levels, hence, we conclude that there is significant  
causal impact; we note that the 5% and 10% significance levels are computed from the test for the absence of Granger  
causality). In the tropical Pacific, the influence of ENSO on evaporation might be associated with Wind–Evaporation SST  
(WES) effect (Cai et al., 2019). The WES effect occurs when warm (cold) water becomes warmer (colder) due to decrease  
110 (increase) in evaporation and weakened (strengthened) surface winds. Besides, ENSO is known to induce changes in global  
precipitation with decrease in rainfall in Africa, Indochina Peninsula, Indonesia, Australia and Amazonia during El Niño  
phase (Dai and Wigley, 2000) and thus indirectly influence evaporation of these regions.

Additional analyses show a more robust influence from ENSO on global evaporation in boreal spring compared to other  
seasons (Figure S2 in the Supplement). The ENSO influence on boreal winter evaporation is mainly found in the tropical  
115 Pacific, while land evaporation is less likely to be influenced by ENSO in winter (Figure S2a). The limited response of  
Northern Hemisphere boreal winter evaporation to ENSO might be related to low energy supply (i.e. incoming solar  
radiation), which leads to reduction in land evaporation (Martens et al., 2018). Although ENSO strength peaks in boreal  
winter, the weak response of evaporation to ENSO during this specific time of the year suggests the important role of other  
internal climate modes or external factors (i.e. solar radiation). The boreal winter evaporation in the Southern Hemisphere  
120 might be controlled by local background conditions (e.g., surface temperature) and other major climate modes (e.g. the  
Southern Annular Mode [SAM]). The response of global evaporation to ENSO is found to be the most robust in boreal  
spring and gradually decrease in summer, fall and winter (Figure S2 and S3). These results indicate the persistent and lagged



influence of ENSO on regional evaporation (e.g., Australia, northeastern South America and tropical Pacific are influenced during boreal spring, summer and fall). The seasonal connection between ENSO and global evaporation in future simulations  
125 (Figure S3) shows similar patterns compared to historical simulations (Figure S2).

### IOD influence on evaporation

Figure 2 describes the evaporation response to the IOD which is mainly found in Indian ocean and the tropical Pacific. The IOD impacts are shown to be significant in the western tropical Indian ocean close to the eastern coast of Africa (Figures 2a and 2b, see Figure S4a for additional details). The evaporation response in the western tropical Indian ocean to the IOD may  
130 be associated with the impact of the IOD on short rains in East Africa (Behera et al., 2006; Black et al., 2003). The IOD signature is also found in the areas close to the Horn of Africa (Figure 2a). This result is in agreement with previous work (Martens et al., 2018) which proposed a possible evaporation response of Horn of Africa to positive phase of the IOD. The IOD shows remote control of evaporation in parts of tropical Pacific, especially the eastern regions (Figure S4b). This teleconnection might be associated with the IOD effects on ENSO and SST in the eastern parts of tropical Pacific (e.g.,  
135 Izumo et al., 2010; Le & Bae, 2019). In historical simulations (Figure 2a), the IOD impacts might reach as far as the Southern Ocean (region close to 150°W to 120°W; 45°S to 60°S) where there is high agreement between models. This IOD-Southern Ocean teleconnection might be indirect and is possibly related to other major climate mode of the Southern Hemisphere (e.g. the SAM).

Although the IOD is shown to contribute to droughts in East Asia (Kripalani et al., 2009) and Australia (Ashok et al., 2003;  
140 Cai et al., 2009; Ummenhofer et al., 2009), our analyses imply that the IOD impacts on evaporation of these regions are unclear, particularly in the future period of 2006-2100 (Figures 2b, S5 and S6). Additionally, there is uncertainty in the impact of the IOD on evaporation in other regions, including the middle East, South Asia, Southeast Asia where there is complex interactions between different climate modes (e.g., ENSO, IOD and the Indian summer monsoon rainfall; Cai et al., 2011; Le & Bae, 2019). Unlike seasonal responses of evaporation to ENSO, the seasonal responses of evaporation to the  
145 IOD indicate similar patterns between different times of the year (Figure S3 and S4). Specifically, in all four seasons, the IOD influence on evaporation is mainly shown in parts of tropical Indian and Pacific oceans. Although there is still uncertainty, IOD signal is found in evaporation change of Amazonia (i.e. northeastern South America, Figures S5a and S6a) in boreal winter (December–February) for several model simulations. These results are in agreement with previous study (Martens et al., 2018) which showed the sensitivity of evaporation in the rainforest to the IOD.

### 150 NAO influence on evaporation

The global evaporation response to NAO, which is limited in the Northern Hemisphere, is shown in Figure 3. NAO mainly contributes to change in evaporation of the North Atlantic European sector where high agreement between models is found (see Figure S7 for additional details). This conclusion shows consistency with earlier works and indicates the capability of models in simulating the connection between NAO and regional evaporation. Particularly, the positive phase of NAO leads



155 to changes in temperature, transport of atmospheric moisture and precipitation in northern, central and western Europe and  
parts of southern Europe and thus causes change in evaporation (Hurrell et al., 2003). Given significant economic losses  
from floods in Europe caused by NAO (Hurrell et al., 2003; Zanardo et al., 2019), the predictability of regional evaporation  
using NAO index might be potentially helpful to mitigate the flood impacts. There is uncertainty of NAO impact on southern  
North Atlantic and eastern Europe. In several models, NAO impact is found in small areas of the eastern tropical Pacific and  
160 South Atlantic (Figure 3a). NAO might also influence evaporation in parts of central North America and the coast of  
northeastern South America; however, these signatures are unclear (Figure 3a). The sensitivity of evaporation in the western  
coast of North America shown in Figure 3a is somewhat in agreement with the findings of previous study (Martens et al.,  
2018).

The seasonal evaporation response to NAO is much weaker in boreal fall and winter compared to spring and summer (Figure  
165 S8 and S9). In the Northern Hemisphere, this result might be due to decrease in seasonal solar radiation. The NAO impacts  
on northwestern Europe in boreal spring (Figure S8b and S9b) suggests several months lagged effect of NAO on evaporation  
of this region. Global evaporation response to NAO is the most robust in boreal spring where NAO signature might exist in  
large area of northern Eurasian continent and parts of Pacific Ocean (Figure S8b).

### Comparing the impacts of different climate modes

170 Figure 4 shows the difference in multi-model mean probability for the absence of Granger causality between a pair of  
climate modes and annual mean evaporation. Specifically, the effects of ENSO on evaporation are more significant  
compared to NAO in large parts of tropical region (highlighted in blue shades which indicate lower probability of no causal  
impacts) while NAO effects are more significant in the high latitude region of Northern Hemisphere (highlighted in red  
shades), especially regarding the North Atlantic European sector (Figures 4a and 4d). We observe stronger signature of  
175 ENSO compared to the IOD in the Middle East, the Pacific coast of North America and large parts of the tropics, except for  
the western tropical Indian Ocean (Figures 4b and 4e). Figure 4e indicates the increase in ENSO spatial impact over the  
western Indian Ocean in the 21<sup>st</sup> century compared to 20<sup>th</sup> century. This increase in ENSO impacts might be related to the  
increase in future extreme ENSO events (Cai et al., 2015). Interestingly, the IOD effects is found slightly stronger compared  
to ENSO in the North Pacific and North Atlantic, suggesting the potential role of the IOD in these regions. The impacts of  
180 NAO are more significant compared to the IOD in the North Atlantic European sector while IOD impacts are stronger in the  
tropical Pacific and Indian Oceans and high latitude region of southern hemisphere (Figures 4c and 4f). Overall, ENSO is the  
dominant mode of tropical evaporation while NAO largely contribute to regional evaporation in the high latitude of Northern  
Hemisphere.

### Discussions

185 The map of ENSO-evaporation connection presented here (Figures 1, S1, S2 and S3) confirm the results obtained previously  
(e.g., ENSO influence on evaporation of Australia and Amazonia where there is high consistency between models as shown



in Figure 1). The results shown here are partly in agreement with previous study (Miralles et al., 2013) which showed lower evaporation during El Niño events due to decrease in precipitation in eastern and central Australia and eastern South America. In addition, the robust signature of ENSO on evaporation of tropical regions is consistent with the findings of  
190 Miralles et al. (2013) which showed negative (positive) anomalies of evaporation for most of the tropics under El Niño (La Niña) conditions. Besides, our results also show new features of the connection between ENSO and global evaporation. Specifically, ENSO is more likely to have influence on the Pacific coasts of both North and South America. The IOD is suggested to be the main climate mode to have impacts on evaporation of both hemispheres (Martens et al., 2018), however, our results indicate that ENSO influence also has similar characteristics (Figures 1, S1 and S2). In addition, there is  
195 uncertainty of ENSO impacts on land evaporation, especially regarding the regions of South Asia, Africa and Southern South America. The result of ENSO influence on eastern Australia shows consistency with past findings (Martens et al., 2018; Miralles et al., 2013), however, we further indicate that there is also close connection between western Australia evaporation and ENSO variations (Figures 1, S1 and S2). In fact, evaporation in Australian continent was shown to have highest sensitivity to ENSO conditions compared to other continents (Miralles et al., 2013). Additionally, our results suggest  
200 that ENSO is more likely to have impacts on evaporation of Australia during both historical period of 1906-2000 and future period 2006-2100. We note that in the present study, we use longer data periods (i.e. 1906-2000 and 2006-2100 model simulations) compared to recent works [e.g., 1982-2012 (Martens et al., 2018) and 1980-2011 (Miralles et al., 2013) observations]. Hence, the length of data period might affect the statistical significance tests and the interpretation of results. There are different factors that might contribute to the ambiguity of climate mode impacts on evaporation of several regions  
205 (e.g. South Asia, Africa and Southern South America). Specifically, these factors include the large discrepancies of current estimations of land evaporation for recent decades (Dong & Dai, 2017; Miralles et al., 2016), the limitations of climate models in simulating climate modes (Gong et al., 2017; Lee et al., 2018; Taschetto et al., 2014; Weller and Cai, 2013) and the overestimation of simulated evaporation in most regions (Mueller and Seneviratne, 2014).

Figure 5 shows the fraction area of Earth surface for land and ocean with probability for the absence of Granger causality  
210 between climate modes and evaporation less than 0.1 (i.e., p value < 0.1; we note that the fraction area is substantially smaller if p value < 0.05). Specifically, during the period 1906-2000, nearly 1.039% of land area is affected by ENSO at 10% significance level while the affected land areas by NAO and the IOD are 0% and 0.017%, respectively (Figure 5a). The area of oceanic evaporation influenced by ENSO, NAO and the IOD are 2.908%, 0.01% and 0.196%, respectively (Figure 5b). We observe an increase in land area affected by ENSO to 1.38% during the 2006-2100 period while the affected land  
215 areas by NAO and the IOD are 0% (Figure 5c). The area of oceanic evaporation influenced by ENSO, NAO and the IOD are 2.944%, 0.003% and 0.122%, respectively (Figure 5d). This result shows a minor decrease in NAO and IOD effects on oceanic evaporation during the 2006-2100 period compared to the 1906-2000 period. Figure S10 shows additional analyses for the fraction area of Earth surface for land and ocean with probability for the absence of Granger causality between climate modes and evaporation less than 0.25 (i.e., climate modes are unlikely to have no causal effects on evaporation;  
220 Stocker et al., 2013).



The considered climate modes (i.e. ENSO, NAO and IOD) are more likely to have influences on global evaporation over oceans while they have limited signature in change of land evaporation for many regions (Figures 1, 2, 3, 5 and S10). These results indicate the role of other factors in modulating land evaporation. Particularly, the influence of major climate modes on land evaporation might be offset by other factors like greenhouse gases, aerosols or solar radiation (Dong and Dai, 2017; Hegerl et al., 2015; Liu et al., 2011). The impacts of climate modes on ocean evaporation contribute to change in global hydrological cycle as ocean evaporation might affect land water cycle by inducing change in regional precipitation (Diawara et al., 2016). For example, the evaporation of the eastern North Pacific is the main moisture supply for precipitation in California (Wei et al., 2016).

Changes in the spatial influences of major modes of climate variability on regional evaporation for future period 2006-2100 and historical period 1906-2000 depend on each climate mode (Figures 1, 2, 3). Analyses in details of the difference between these two periods are shown in Figure 6. Specifically, the fraction area of Earth surface showing lower probability of ENSO effects for 2006-2100 period is approximately 52.9% (Figure 6a). This result indicates that ENSO slightly expand the impacted regions (highlighted in red shades, Figure 6a) during 2006-2100 period compared to 1906-2000 period. Conversely, the fraction area of Earth surface for effects of NAO and the IOD during the 2006-2100 period are decreased with 47.2% and 45.7%, respectively (Figure 6b and 6c). These results suggest that, for several regions of declining impacts of climate modes (highlighted in blue shades, Figure 6), evaporation processes in the 21<sup>st</sup> century tend to involve more local climate background conditions (e.g., precipitation, near-surface air temperature, wind speed, soil moisture). For example, response of regional evaporation to climate warming depends on precipitation (Parr et al., 2016; Zhang et al., 2018) and projected rise of surface temperature is shown to mainly contribute to the increase in regional evaporation (Láiné et al., 2014). Because the volume of moisture carried by air increases with air temperature, the atmospheric water vapor demand is expected to increase with rising air temperature and rising greenhouse gases concentration (Miralles et al., 2013). In addition, the declines in pan evaporation in southern/western Australia are mainly caused by decreases in wind speeds (Stephens et al., 2018).

#### 4 Conclusions

The CMIP5 historical and RCP8.5 future simulations provide an opportunity to assess the influence of major climate modes on global evaporation, which plays an important role in hydrological cycle, drought monitoring and water resources management. This paper employed tests of Granger causality and showed vigorous evaluation of possible impacts of NAO, the IOD and ENSO on global evaporation.

The results show that ENSO is likely to have impacts on evaporation of different regions in both hemispheres, including tropical Pacific and Indian Oceans, Indochina Peninsula, middle Asia (regions closed to Caspian Sea), Australia, northeastern South America (i.e. Amazonia) and the Pacific coast of North and South America. The impacts of NAO are mainly found in the North Atlantic and European regions while the notable influence of the IOD is limited in western



tropical Indian Ocean and part of eastern tropical Pacific. Despite more extreme IOD events are expected in the future (Cai et al., 2013, 2014), the spatial influences of the IOD on evaporation are slightly less significant in the 2006-2100 period compared to the 1906-2000 period. The weak impacts of ENSO, NAO and the IOD on evaporation of several regions suggest the importance of external forcings (e.g. greenhouse gases radiative forcing, solar forcing) and other climate modes on global evaporation variability. We emphasize the strong connection between considered climate modes (i.e. ENSO, IOD and NAO) and oceanic evaporation at interannual time scales. Land evaporation is shown to have weak connection with teleconnection indices in several regions, suggesting the important role of local wind speed (Stephens et al., 2018), surface temperature (Lainé et al., 2014; Miralles et al., 2013), moisture supply (Jung et al., 2010) and amount of precipitation (Parr et al., 2016) on changes in land evaporation.

Our results may have suggestions for the predictability of regional evaporation (e.g. Australia, tropical Pacific, tropical Indian and North Atlantic Oceans, the Pacific coast of North and South America, Amazonia, Europe, Indochina Peninsula and middle Asia) by using past time series of major climate modes for short term of several years. The results of this study might provide information for drought and flood prediction as evaporation is an important metric for quantifying drought (McEvoy et al., 2016) and flood events.

Uncertainty regarding the impact of major climate modes on evaporation of several regions (e.g. ENSO impacts on evaporation of South Asia, South Africa, eastern North America, southern South America; the IOD impacts on western Africa and South Asia; NAO impacts on North Atlantic and surrounding areas) suggests that additional works are necessary. Further investigation about the effects of other internal climate modes (e.g., the Southern Annular Mode [SAM], the Indian Ocean Basin [IOB] mode, the North Tropical Atlantic [NTA]) on evaporation might improve our understanding of the response global hydrological cycle to internal climate variability. Little effort has been made to quantify the influences of external climate factors (i.e., volcanic eruptions, solar variations, and changes in concentration of greenhouse gases) on global evaporation, thus, these analyses might be a subject of forthcoming studies.

## 275 **Data availability**

CMIP data can be downloaded from the ESGF website at <https://esgf-node.llnl.gov/projects/esgf-llnl/>.

## **Competing interests**

The authors declare that they have no conflict of interest.



### Author contribution

- 280 TL designed the study. TL performed the data analysis and wrote the manuscript. DHB contributed to the interpretation of results and the writing of manuscript.

### Acknowledgements

- We thank Ryan Teuling for valuable comments and suggestions. We acknowledge the World Climate Research Programme's Working Group on Coupled Modeling, which is responsible for CMIP, and we thank the climate modeling groups (listed in  
285 Table S1 of this paper) for producing and making available their model output. For CMIP the U.S. Department of Energy's Program for Climate Model Diagnosis and Intercomparison provided coordinating support and led the development of software infrastructure in partnership with the Global Organization for Earth System Science Portals. T. Le is supported by a research grant from Sejong University. This work is supported by the Korea Environmental Industry and Technology Institute (KEITI); the research grant is funded by the Ministry of Environment (grant RE201901084).

### 290 References

- Arora, A., Rao, S. A., Chattopadhyay, R., Goswami, T., George, G. and Sabeerali, C. T.: Role of Indian Ocean SST variability on the recent global warming hiatus, *Glob. Planet. Change*, 143, 21–30, doi:10.1016/j.gloplacha.2016.05.009, 2016.
- Ashok, K., Guan, Z. and Yamagata, T.: Influence of the Indian Ocean Dipole on the Australian winter rainfall, *Geophys. Res. Lett.*, 30(15), 3–6, doi:10.1029/2003GL017926, 2003.
- 295 Behera, S. K., Luo, J. J., Masson, S., Rao, S. a., Sakuma, H. and Yamagata, T.: A CGCM study on the interaction between IOD and ENSO, *J. Clim.*, 19(9), 1688–1705, doi:10.1175/JCLI3797.1, 2006.
- Bjerknes, J.: Atmospheric Teleconnections From the Equatorial Pacific, *Mon. Weather Rev.*, 97(3), 163–172, doi:10.1175/1520-0493(1969)097<0163:ATFTEP>2.3.CO;2, 1969.
- 300 Black, E., Slingo, J. M. and Sperber, K. R.: An observational study of the relationship between excessively strong short rains in coastal East Africa and Indian Ocean SST., *Mon. Weather Rev.*, 74–94, doi:10.1175/1520-0493(2003)131<0074:AOSOTR>2.0.CO;2, 2003.
- Cai, W., Cowan, T. and Sullivan, a.: Recent unprecedented skewness towards positive Indian Ocean Dipole occurrences and its impact on Australian rainfall, *Geophys. Res. Lett.*, 36(11), 1–4, doi:10.1029/2009GL037604, 2009.
- 305 Cai, W., Sullivan, A. and Cowan, T.: Interactions of ENSO, the IOD, and the SAM in CMIP3 models, *J. Clim.*, 24(6), 1688–1704, doi:10.1175/2010JCLI3744.1, 2011.
- Cai, W., Zheng, X.-T., Weller, E., Collins, M., Cowan, T., Lengaigne, M., Yu, W. and Yamagata, T.: Projected response of the Indian Ocean Dipole to greenhouse warming, *Nat. Geosci.*, 6(12), 999–1007, doi:10.1038/ngeo2009, 2013.
- 310 Cai, W., Santoso, A., Wang, G., Weller, E., Wu, L., Ashok, K., Masumoto, Y. and Yamagata, T.: Increased frequency of extreme Indian Ocean Dipole events due to greenhouse warming., *Nature*, 510(7504), 254–8, doi:10.1038/nature13327, 2014.



- Cai, W., Wang, G., Santoso, A., McPhaden, M. J., Wu, L., Jin, F.-F., Timmermann, A., Collins, M., Vecchi, G., Lengaigne, M., England, M. H., Dommenges, D., Takahashi, K. and Guilyardi, E.: Increased frequency of extreme La Niña events under greenhouse warming, *Nat. Clim. Chang.*, 5(2), 132–137, doi:10.1038/nclimate2492, 2015.
- 315 Cai, W., Wu, L., Lengaigne, M., Li, T., McGregor, S., Kug, J.-S., Yu, J.-Y., Stuecker, M. F., Santoso, A., Li, X., Ham, Y.-G., Chikamoto, Y., Ng, B., McPhaden, M. J., Du, Y., Dommenges, D., Jia, F., Kajtar, J. B., Keenlyside, N., Lin, X., Luo, J.-J., Martín-Rey, M., Ruprich-Robert, Y., Wang, G., Xie, S.-P., Yang, Y., Kang, S. M., Choi, J.-Y., Gan, B., Kim, G.-I., Kim, C.-E., Kim, S., Kim, J.-H. and Chang, P.: Pantropical climate interactions, *Science* (80-. ), 363, doi:10.1126/SCIENCE.AAV4236, 2019.
- 320 Cavusoglu, A. H., Chen, X., Gentile, P. and Sahin, O.: Potential for natural evaporation as a reliable renewable energy resource, *Nat. Commun.*, 8(1), doi:10.1038/s41467-017-00581-w, 2017.
- Cheng, L., Zhang, L., Wang, Y. P., Canadell, J. G., Chiew, F. H. S., Beringer, J., Li, L., Miralles, D. G., Piao, S. and Zhang, Y.: Recent increases in terrestrial carbon uptake at little cost to the water cycle, *Nat. Commun.*, 8(1), doi:10.1038/s41467-017-00114-5, 2017.
- 325 Chu, J. E., Ha, K. J., Lee, J. Y., Wang, B., Kim, B. H. and Chung, C. E.: Future change of the Indian Ocean basin-wide and dipole modes in the CMIP5, *Clim. Dyn.*, 43(1–2), 535–551, doi:10.1007/s00382-013-2002-7, 2014.
- Dai, A. and Wigley, T. M. L.: Global patterns of ENSO-induced precipitation., *Geophys. Res. Lett.*, 27(9), 1283–1286, 2000.
- Diawara, A., Tachibana, Y., Oshima, K., Nishikawa, H. and Ando, Y.: Synchrony of trend shifts in Sahel boreal summer rainfall and global oceanic evaporation, 1950–2012, *Hydrol. Earth Syst. Sci.*, 20(9), 3789–3798, doi:10.5194/hess-20-3789-2016, 2016.
- 330 Dong, B. and Dai, A.: The uncertainties and causes of the recent changes in global evapotranspiration from 1982 to 2010, *Clim. Dyn.*, 49(1–2), 279–296, doi:10.1007/s00382-016-3342-x, 2017.
- Friedrich, K., Grossman, R. L., Huntington, J., Blanken, P. D., Lenters, J., Holman, K. D., Gochis, D., Livneh, B., Prairie, J., Skeie, E., Healey, N. C., Dahm, K., Pearson, C., Fennessey, T., Hook, S. J. and Kowalski, T.: Reservoir Evaporation in the Western United States: Current Science, Challenges, and Future Needs, *Bull. Am. Meteorol. Soc.*, 99(1), 167–187, doi:10.1175/BAMS-D-15-00224.1, 2018.
- 335 Gong, H., Wang, L., Chen, W., Chen, X. and Nath, D.: Biases of the wintertime Arctic Oscillation in CMIP5 models, *Environ. Res. Lett.*, 12(1), doi:10.1088/1748-9326/12/1/014001, 2017.
- Hegerl, G. C., Black, E., Allan, R. P., Ingram, W. J., Polson, D., Trenberth, K. E. . . . and Zhang, X.: Challenges in Quantifying Changes in the Global Water Cycle, *Bull. Am. Meteorol. Soc.*, 2015.
- 340 Hurrell, J. W., Kushnir, Y., Ottersen, G. and Visbeck, M.: An Overview of the North Atlantic Oscillation, in *The North Atlantic Oscillation: Climate Significance and Environmental Impact*, pp. 1–35, American Geophysical Union., 2003.
- Izumo, T., Vialard, J., Lengaigne, M., de Boyer Montegut, C., Behera, S. K., Luo, J.-J., Cravatte, S., Masson, S. and Yamagata, T.: Influence of the state of the Indian Ocean Dipole on the following year’s El Niño, *Nat. Geosci.*, 3(3), 168–172, doi:10.1038/ngeo760, 2010.
- 345 Jung, M., Reichstein, M., Ciais, P., Seneviratne, S. I., Sheffield, J., Goulden, M. L., Bonan, G., Cescatti, A., Chen, J., de Jeu, R., Dolman, A. J., Eugster, W., Gerten, D., Gianelle, D., Gobron, N., Heinke, J., Kimball, J., Law, B. E., Montagnani, L., Mu, Q., Mueller, B., Oleson, K., Papale, D., Richardson, A. D., Rouspard, O., Running, S., Tomelleri, E., Viovy, N., Weber, U., Williams, C., Wood, E., Zaehle, S. and Zhang, K.: Recent decline in the global land evapotranspiration trend due to limited moisture supply, *Nature*, 467(7318), 951–954, doi:10.1038/nature09396, 2010.
- 350 Kitoh, A.: The Asian Monsoon and its Future Change in Climate Models: A Review, *J. Meteorol. Soc. Japan. Ser. II*, 95(1), 7–33, doi:10.2151/jmsj.2017-002, 2016.



- Kripalani, R. H., Oh, J. H. and Chaudhari, H. S.: Delayed influence of the Indian Ocean Dipole mode on the East Asia-West Pacific monsoon: possible mechanism, *Int. J. Climatol.*, 30(2), n/a-n/a, doi:10.1002/joc.1890, 2009.
- 355 Laîné, A., Nakamura, H., Nishii, K. and Miyasaka, T.: A diagnostic study of future evaporation changes projected in CMIP5 climate models, *Clim. Dyn.*, 42(9–10), 2745–2761, doi:10.1007/s00382-014-2087-7, 2014.
- Le, T.: Solar forcing of Earth's surface temperature in PMIP3 simulations of the last millennium, *Atmos. Sci. Lett.*, 16(3), 285–290, doi:10.1002/asl2.555, 2015.
- 360 Le, T. and Bae, D.-H.: Causal links on interannual timescale between ENSO and the IOD in CMIP5 future simulations, *Geophys. Res. Lett.*, 46(5), 2820–2828, doi:10.1029/2018GL081633, 2019.
- Le, T., Sjolte, J. and Muscheler, R.: The influence of external forcing on subdecadal variability of regional surface temperature in CMIP5 simulations of the last millennium, *J. Geophys. Res. Atmos.*, 121(4), 1671–1682, doi:10.1002/2015JD024423, 2016.
- 365 Lee, J., Sperber, K. R., Gleckler, P. J., Bonfils, C. J. W. and Taylor, K. E.: Quantifying the agreement between observed and simulated extratropical modes of interannual variability, Springer Berlin Heidelberg., 2018.
- Lee, M. H., Im, E. S. and Bae, D. H.: A comparative assessment of climate change impacts on drought over Korea based on multiple climate projections and multiple drought indices, *Clim. Dyn.*, 0(0), 0, doi:10.1007/s00382-018-4588-2, 2019.
- Leung, M. Y. T. and Zhou, W.: Direct and indirect ENSO modulation of winter temperature over the Asian-Pacific-American region, *Sci. Rep.*, 6(October), 1–7, doi:10.1038/srep36356, 2016.
- 370 Liu, X., Luo, Y., Zhang, D., Zhang, M. and Liu, C.: Recent changes in pan-evaporation dynamics in China, *Geophys. Res. Lett.*, 38(13), 10–13, doi:10.1029/2011GL047929, 2011.
- Martens, B., Waegeman, W., Dorigo, W. A., Verhoest, N. E. C. and Miralles, D. G.: Terrestrial evaporation response to modes of climate variability, *npj Clim. Atmos. Sci.*, 1(1), 43, doi:10.1038/s41612-018-0053-5, 2018.
- 375 McEvoy, D. J., Huntington, J. L., Mejia, J. F. and Hobbins, M. T.: Improved seasonal drought forecasts using reference evapotranspiration anomalies, *Geophys. Res. Lett.*, 43(1), 377–385, doi:10.1002/2015GL067009, 2016.
- Miralles, D. G., Van Den Berg, M. J., Teuling, A. J. and De Jeu, R. A. M.: Soil moisture-temperature coupling: A multiscale observational analysis, *Geophys. Res. Lett.*, 39(21), 2–7, doi:10.1029/2012GL053703, 2012.
- 380 Miralles, D. G., van den Berg, M. J., Gash, J. H., Parinussa, R. M., de Jeu, R. a. M., Beck, H. E., Holmes, T. R. H., Jiménez, C., Verhoest, N. E. C., Dorigo, W. a., Teuling, A. J. and Johannes Dolman, A.: El Niño–La Niña cycle and recent trends in continental evaporation, *Nat. Clim. Chang.*, 4(1), 1–5, doi:10.1038/nclimate2068, 2013.
- Miralles, D. G., Jiménez, C., Jung, M., Michel, D., Ershadi, A., McCabe, M. F., Hirschi, M., Martens, B., Dolman, A. J., Fisher, J. B., Mu, Q., Seneviratne, S. I., Wood, E. F. and Fernández-Prieto, D.: The WACMOS-ET project - Part 2: Evaluation of global terrestrial evaporation data sets, *Hydrol. Earth Syst. Sci.*, 20(2), 823–842, doi:10.5194/hess-20-823-2016, 2016.
- 385 Mosedale, T. J., Stephenson, D. B., Collins, M. and Mills, T. C.: Granger causality of coupled climate processes: Ocean feedback on the North Atlantic Oscillation, *J. Clim.*, 1182–1194 [online] Available from: <http://journals.ametsoc.org/doi/abs/10.1175/JCLI3653.1> (Accessed 17 January 2014), 2006.
- Mueller, B. and Seneviratne, S. I.: Systematic land climate and evapotranspiration biases in CMIP5 simulations, *Geophys. Res. Lett.*, 41(1), 128–134, doi:10.1002/2013GL058055, 2014.
- 390 Naumann, G., Alfieri, L., Wyser, K., Mentaschi, L., Betts, R. A., Carrao, H., Spinoni, J., Vogt, J. and Feyen, L.: Global Changes in Drought Conditions Under Different Levels of Warming, *Geophys. Res. Lett.*, 45(7), 3285–3296, doi:10.1002/2017GL076521, 2018.

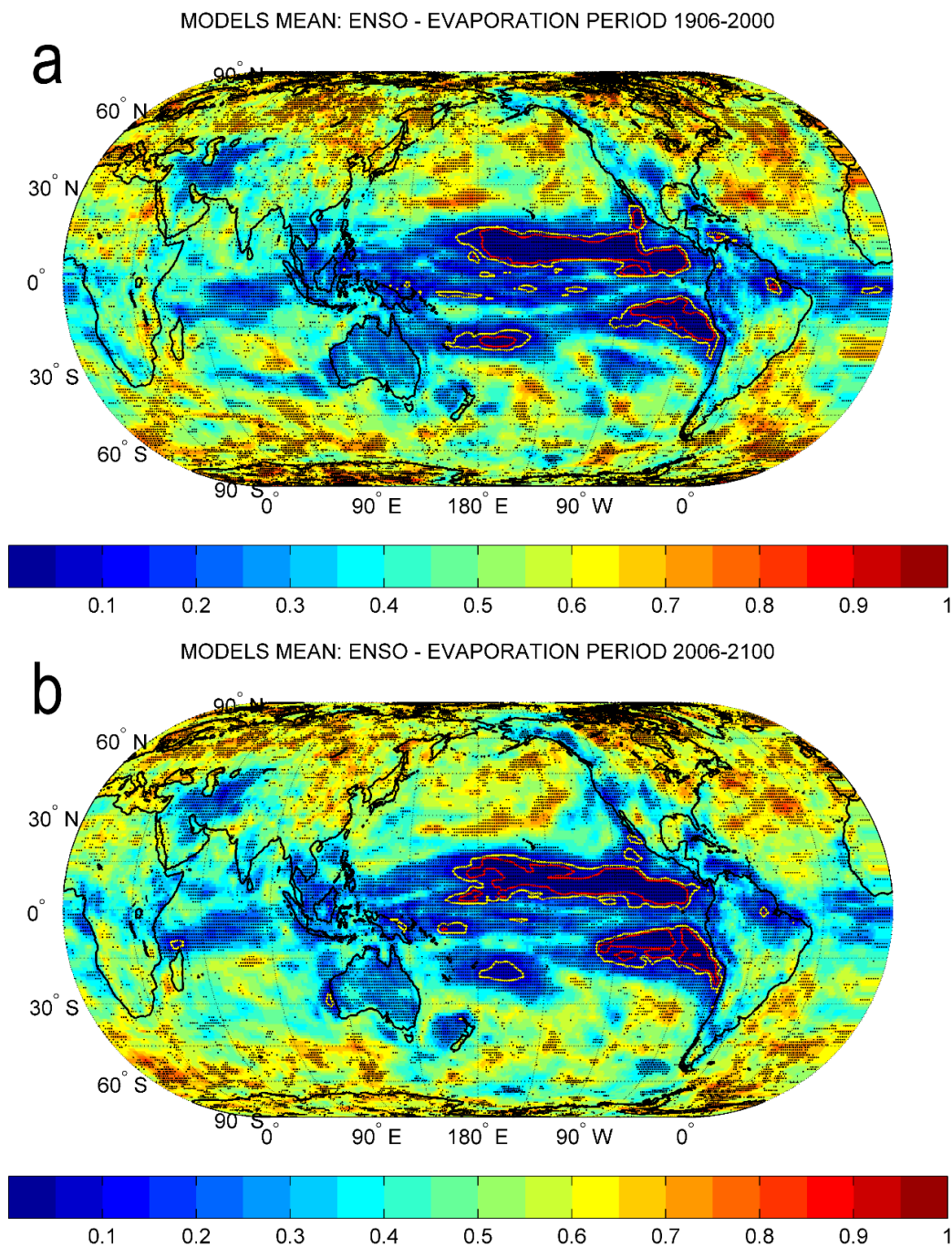


- Neelin, J. D., Battisti, D. S., Hirst, A. C., Jin, F.-F., Wakata, Y., Yamagata, T. and Zebiak, S. E.: ENSO theory, *J. Geophys. Res.*, 103(C7), 14261, doi:10.1029/97JC03424, 1998.
- 395 Nicolai-Shaw, N., Gudmundsson, L., Hirschi, M. and Seneviratne, S. I.: Long-term predictability of soil moisture dynamics at the global scale: Persistence versus large-scale drivers, *Geophys. Res. Lett.*, 43(16), 8554–8562, doi:10.1002/2016GL069847, 2016.
- Van Osnabrugge, B., Uijlenhoet, R. and Weerts, A.: Contribution of potential evaporation forecasts to 10-day streamflow forecast skill for the Rhine River, *Hydrol. Earth Syst. Sci.*, 23(3), 1453–1467, doi:10.5194/hess-23-1453-2019, 2019.
- 400 Parr, D., Wang, G. and Fu, C.: Understanding evapotranspiration trends and their driving mechanisms over the NLDAS domain based on numerical experiments using CLM4.5, *J. Geophys. Res. Atmos.*, doi:10.1002/2016JD025137. Received, 2016.
- Saji, N. H., Vinayachandran, P. N. and Yamagata, T.: A dipole in the tropical Indian Ocean, *Nature*, 401(September), 360–363, 1999.
- 405 Son, K. H. and Bae, D. H.: Drought analysis according to shifting of climate zones to arid climate zone over Asia monsoon region, *J. Hydrol.*, 529, 1021–1029, doi:10.1016/j.jhydrol.2015.09.010, 2015.
- Stephens, C. M., McVicar, T. R., Johnson, F. M. and Marshall, L. A.: Revisiting Pan Evaporation Trends in Australia a Decade on, *Geophys. Res. Lett.*, 45(20), 11,164–11,172, doi:10.1029/2018GL079332, 2018.
- 410 Stocker, T. F., Qin, G.-K., Plattner, L. V., Alexander, S. K., Allen, N. L., Bindoff, F.-M., Bréon, J. a., Church, U., Cubasch, S., Emori, P., Forster, P., Friedlingstein, N., Gillett, J. M., Gregory, D. L., Hartmann, E., Jansen, B., Kirtman, R., Knutti, K., Krishna Kumar, P., Lemke, J., Marotzke, V., Masson-Delmotte, G. a., Meehl, I. I., Mokhov, S., Piao, V., Ramaswamy, D., Randall, M., Rhein, M., Rojas, C., Sabine, D., Shindell, L. D., Talley, D. G. and Xie, V. and S.-P.: Technical Summary, *Clim. Chang. 2013 Phys. Sci. Basis. Contrib. Work. Gr. I to Fifth Assess. Rep. Intergov. Panel Clim. Chang.*, 33–115, doi:10.1017/CBO9781107415324.005, 2013.
- 415 Sun, C., Li, J. and Ding, R.: Strengthening relationship between ENSO and western Russian summer surface temperature, *Geophys. Res. Lett.*, 43(2), 843–851, doi:10.1002/2015GL067503, 2016.
- Taschetto, A. S., Gupta, A. Sen, Jourdain, N. C., Santoso, A., Ummenhofer, C. C. and England, M. H.: Cold tongue and warm pool ENSO Events in CMIP5: Mean state and future projections, *J. Clim.*, 27(8), 2861–2885, doi:10.1175/JCLI-D-13-00437.1, 2014.
- 420 Taylor, K. E., Stouffer, R. J. and Meehl, G. A.: An Overview of CMIP5 and the Experiment Design, *Bull. Am. Meteorol. Soc.*, 93(4), 485–498, doi:10.1175/BAMS-D-11-00094.1, 2012.
- Teuling, A. J., Taylor, C. M., Meirink, J. F., Melsen, L. A., Miralles, D. G., Van Heerwaarden, C. C., Vautard, R., Stegehuis, A. I., Nabuurs, G. J. and De Arellano, J. V. G.: Observational evidence for cloud cover enhancement over western European forests, *Nat. Commun.*, 8, 1–7, doi:10.1038/ncomms14065, 2017.
- 425 Thirumalai, K., DInezio, P. N., Okumura, Y. and Deser, C.: Extreme temperatures in Southeast Asia caused by El Niño and worsened by global warming, *Nat. Commun.*, 8, 1–8, doi:10.1038/ncomms15531, 2017.
- Ummenhofer, C. C., England, M. H., McIntosh, P. C., Meyers, G. a., Pook, M. J., Risbey, J. S., Gupta, A. Sen and Taschetto, A. S.: What causes southeast Australia’s worst droughts?, *Geophys. Res. Lett.*, 36(4), 1–5, doi:10.1029/2008GL036801, 2009.
- 430 Wang, K. and Dickinson, R. E.: A review of global terrestrial evapotranspiration: Observation, modeling, climatology, and climatic variability, *Rev. Geophys.*, 50(2011), 1–54, doi:10.1029/2011RG000373.1. INTRODUCTION, 2012.
- Wang, X., Li, J., Sun, C. and Liu, T.: NAO and its relationship with the Northern Hemisphere mean surface temperature in CMIP5 simulations, *J. Geophys. Res.*, 122(8), 4202–4227, doi:10.1002/2016JD025979, 2017.

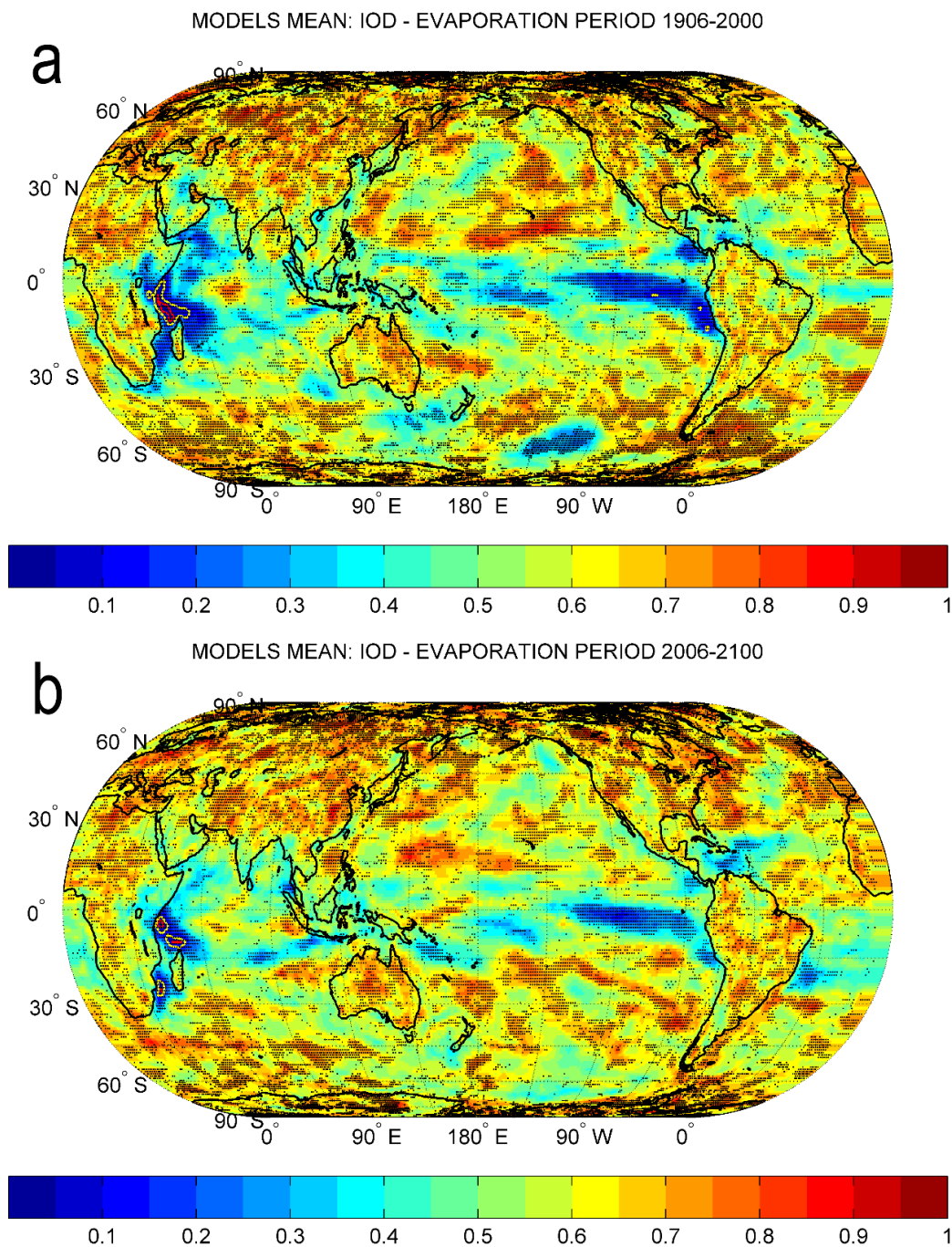


- 435 Webster, P. J., Moore, a M., Loschnigg, J. P. and Leben, R. R.: Coupled ocean-atmosphere dynamics in the Indian Ocean during 1997-98., *Nature*, 401(6751), 356–360, doi:10.1038/43848, 1999.
- Wei, J., Jin, Q., Yang, Z. L. and Dirmeyer, P. A.: Role of ocean evaporation in California droughts and floods, *Geophys. Res. Lett.*, 43(12), 6554–6562, doi:10.1002/2016GL069386, 2016.
- Weller, E. and Cai, W.: Realism of the indian ocean dipole in CMIP5 models: The implications for climate projections, *J. Clim.*, 26(17), 6649–6659, doi:10.1175/JCLI-D-12-00807.1, 2013.
- 440 Xing, W., Wang, W., Shao, Q., Yu, Z., Yang, T. and Fu, J.: Periodic fluctuation of reference evapotranspiration during the past five decades: Does Evaporation Paradox really exist in China?, *Sci. Rep.*, 6(August), 1–12, doi:10.1038/srep39503, 2016.
- 445 Yeh, S. W., Cai, W., Min, S. K., McPhaden, M. J., Dommenges, D., Dewitte, B., Collins, M., Ashok, K., An, S. Il, Yim, B. Y. and Kug, J. S.: ENSO Atmospheric Teleconnections and Their Response to Greenhouse Gas Forcing, *Rev. Geophys.*, 56(1), 185–206, doi:10.1002/2017RG000568, 2018.
- Zanardo, S., Nicotina, L., Hilberts, A. G. J. and Jewson, S. P.: Modulation of Economic Losses From European Floods by the North Atlantic Oscillation, *Geophys. Res. Lett.*, 2563–2572, doi:10.1029/2019GL081956, 2019.
- Zhang, Q., Yang, Z., Hao, X. and Yue, P.: Conversion features of evapotranspiration responding to climate warming in transitional climate regions in northern China, *Clim. Dyn.*, doi:10.1360/N972017-00817, 2018.

450



455 **Figure 1.** Multi-model mean probability map for the absence of Granger causality between ENSO and annual mean evaporation for the periods 1906-2000 (a) and 2006-2100 (b). Stippling demonstrates that at least 70% of models show agreement on the mean probability of all models at given grid point. An individual model's agreement is determined when the difference between the multi-model mean probability and the selected model's probability is less than one standard deviation of multi-model mean probability. The yellow (red) contour line designates  $p$  value = 0.1 (0.05). Blue shades indicate low probability for the absence of Granger causality. ENSO = El Niño–Southern Oscillation.



460 **Figure 2.** As in Figure 1, but for Granger causality between IOD and annual mean evaporation. IOD = Indian Ocean Dipole.

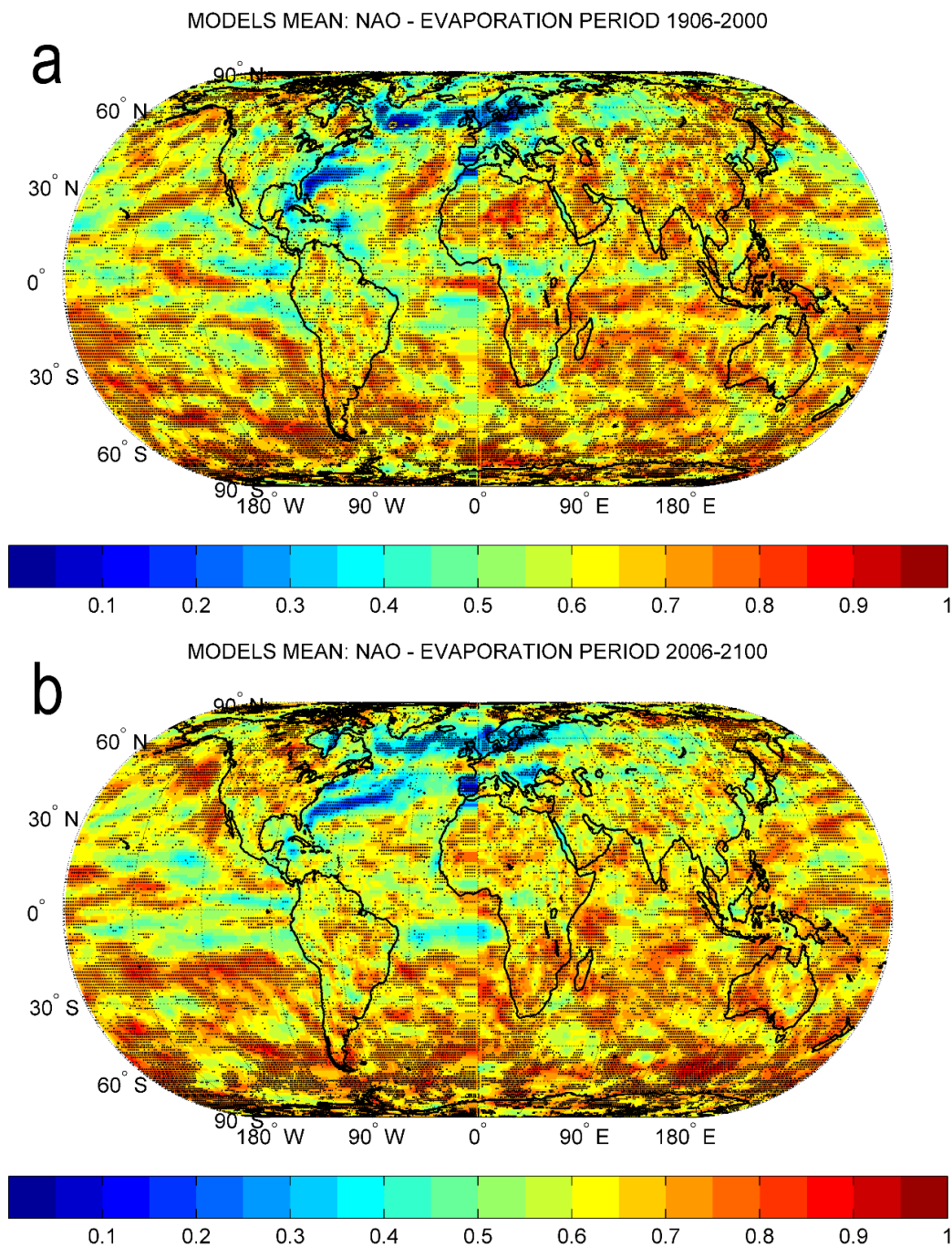
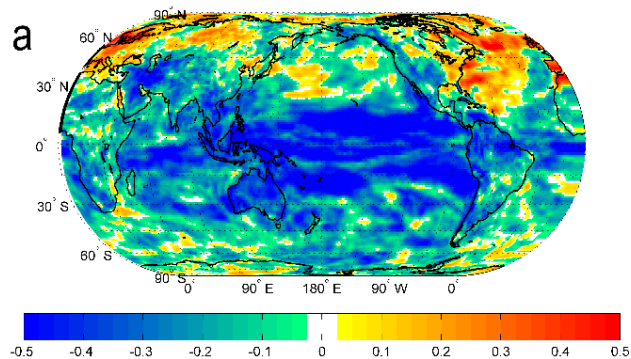


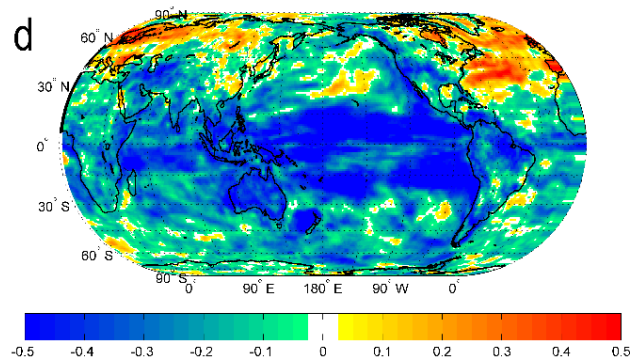
**Figure 3.** As in Figure 1, but for Granger causality between NAO and annual mean evaporation. NAO = North Atlantic Oscillation.



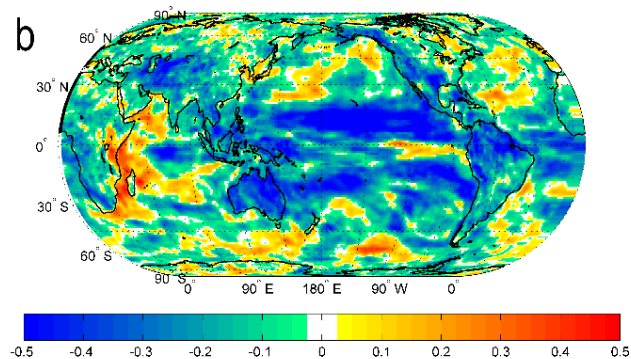
MODELS MEAN OF DIFFERENCE BETWEEN ENSO AND NAO - EVAPORATION: PERIOD 1906-2000



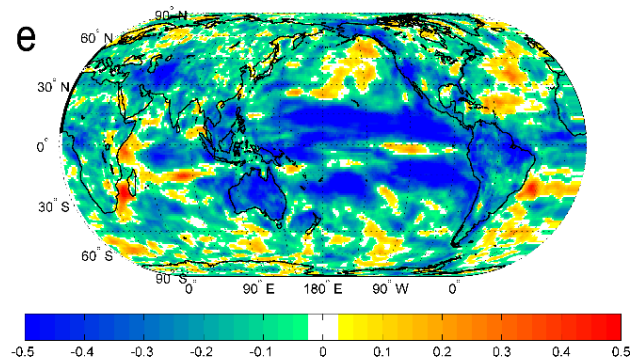
MODELS MEAN OF DIFFERENCE BETWEEN ENSO AND NAO - EVAPORATION: PERIOD 2006-2100



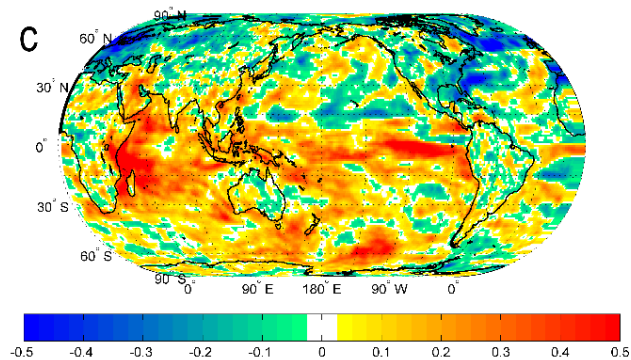
MODELS MEAN OF DIFFERENCE BETWEEN ENSO AND IOD - EVAPORATION: PERIOD 1906-2000



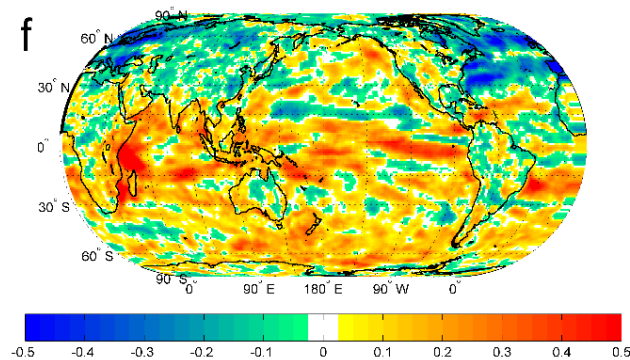
MODELS MEAN OF DIFFERENCE BETWEEN ENSO AND IOD - EVAPORATION: PERIOD 2006-2100



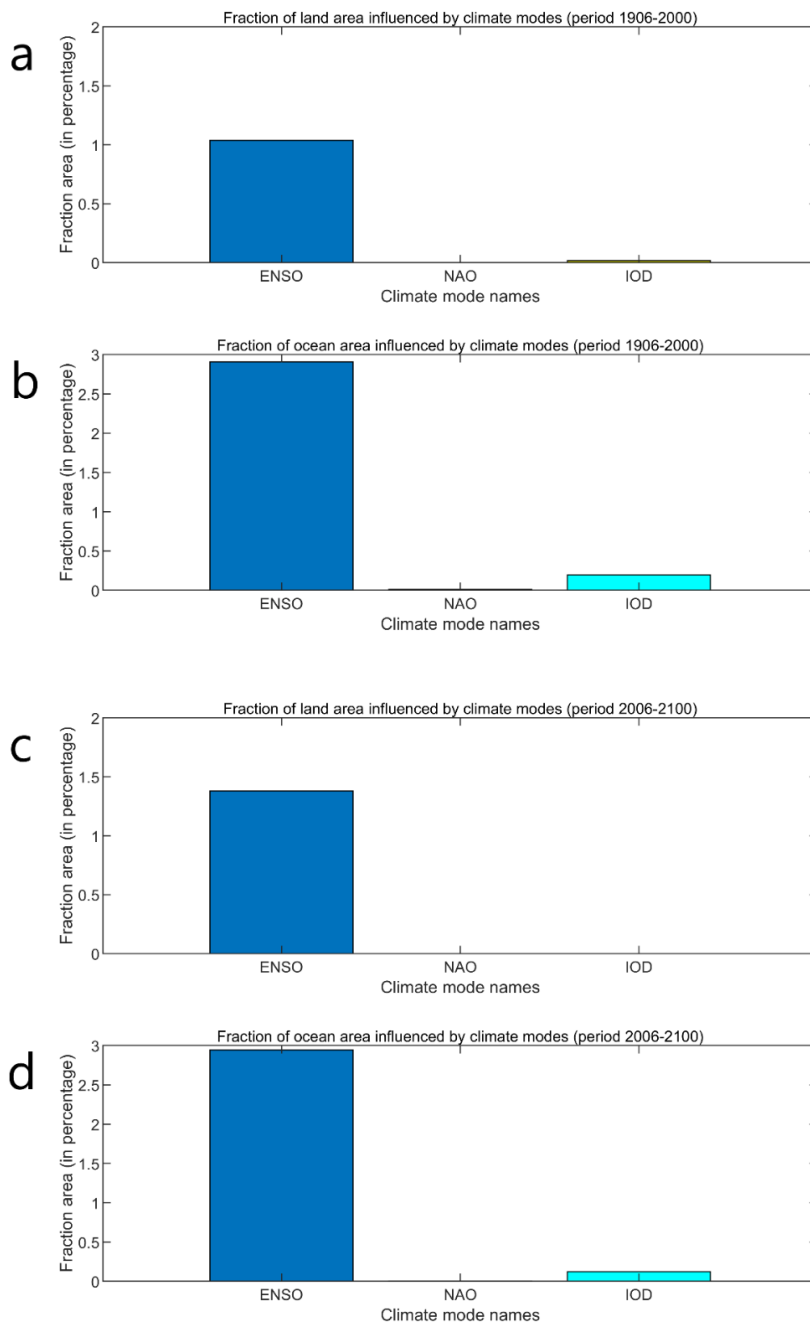
MODELS MEAN OF DIFFERENCE BETWEEN NAO AND IOD - EVAPORATION: PERIOD 1906-2000



MODELS MEAN OF DIFFERENCE BETWEEN NAO AND IOD - EVAPORATION: PERIOD 2006-2100



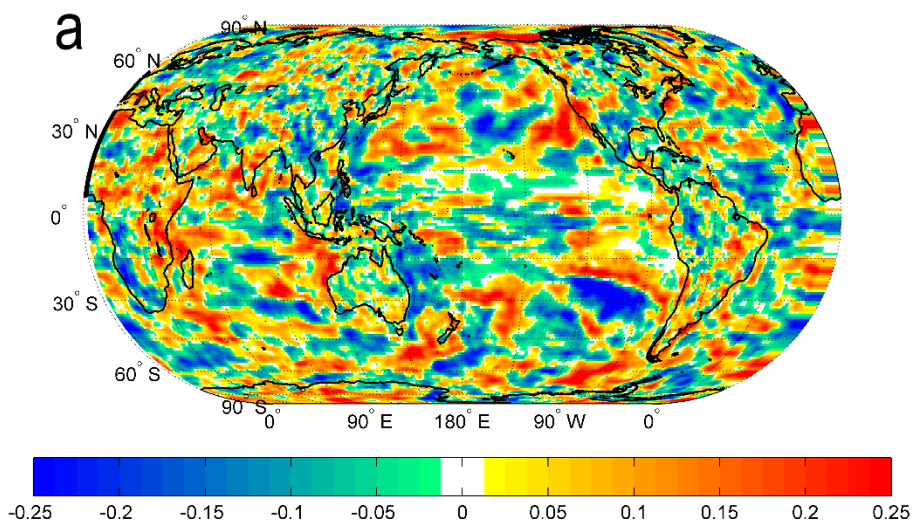
465 **Figure 4.** Difference in multi-model mean probability for the absence of Granger causality between a pair of climate modes and annual mean evaporation. The results are shown for the periods 1906-2000 (a, b, c) and 2006-2100 (d, e, f). ENSO minus NAO (a, d). ENSO minus IOD (b, e). NAO minus IOD (c, f). Blue shades indicate lower probability for the absence of Granger causality. ENSO = El Niño–Southern Oscillation. NAO = North Atlantic Oscillation. IOD = Indian Ocean Dipole.



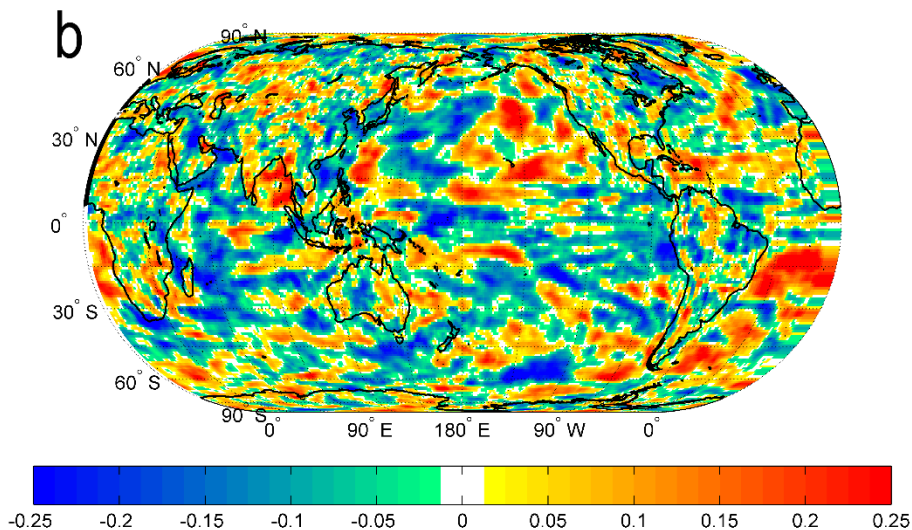
470 **Figure 5.** Fraction of Earth surface for land (a, c) and ocean (b, d) with probability for the absence of Granger causality between climate modes and evaporation less than 0.1 (i.e.,  $p$  value  $< 0.1$ ). The results are shown for the influence of individual climate mode on annual mean evaporation for periods 1906-2000 (a, b) and 2006-2100 (c, d). Fraction area lower than 0.05% is plotted in yellow bar. Fraction area higher than 0.05% and lower than 0.5% is plotted in cyan bar. ENSO = El Niño–Southern Oscillation. NAO = North Atlantic Oscillation. IOD = Indian Ocean Dipole.



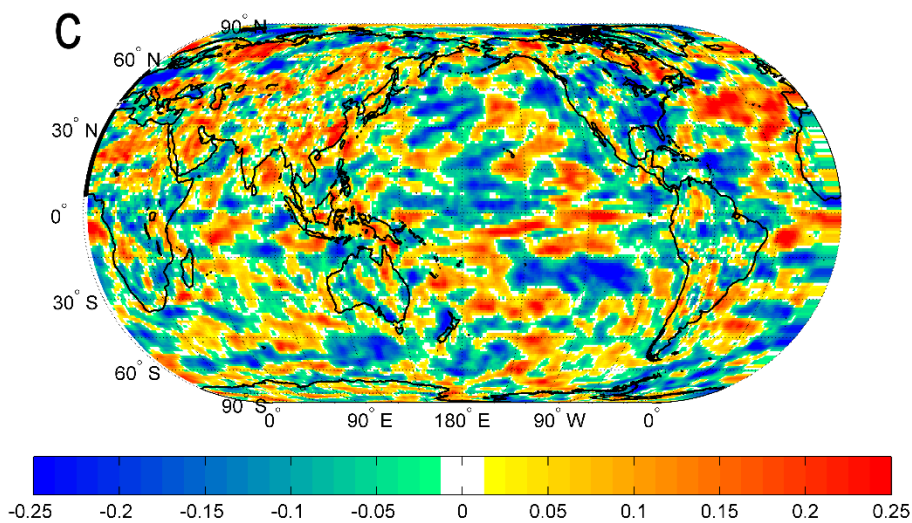
MODELS MEAN OF ENSO - EVAPORATION: PERIOD 1906-2000 MINUS PERIOD 2006-2100



MODELS MEAN OF IOD - EVAPORATION: PERIOD 1906-2000 MINUS PERIOD 2006-2100



MODELS MEAN OF NAO - EVAPORATION: PERIOD 1906-2000 MINUS PERIOD 2006-2100





475 **Figure 6.** Difference of probability for the absence of Granger causality of individual climate mode on annual mean evaporation between periods 1906-2000 and 2006-2100 (i.e., period 1906-2000 minus period 2006-2100). The results are shown for ENSO (a), IOD (b) and NAO (c). Blue shades indicate lower probability of no Granger causality during period 1906-2000 compared to period 2006-2100. Red shades indicate lower probability of no Granger causality during period 2006-2100 compared to period 1906-2000. ENSO = El Niño–Southern Oscillation. NAO = North Atlantic Oscillation. IOD = Indian Ocean Dipole.

480